

## Comparisons of SSM/I Liquid Water Paths with Aircraft Measurements

STEWART G. COBER, ANDRE TREMBLAY, AND GEORGE A. ISAAC

*Cloud Physics Research Division, Atmospheric Environment Service, Downsview, Ontario, Canada*

(Manuscript received 28 February 1995, in final form 3 August 1995)

### ABSTRACT

Comparisons have been made between in situ aircraft measurements of integrated liquid water and retrievals of integrated liquid water path (LWP) from algorithms using SSM/I brightness temperatures. The aircraft measurements were made over the North Atlantic Ocean during the winter of 1992. Six case studies are presented from which trends in the LWP algorithms are discussed. SSM/I liquid water path validation has previously only been performed through comparisons with measurements from upward-looking radiometers or with calculations from radiative transfer models. The case studies presented here reflect an alternative technique for validation.

Aircraft-derived liquid water paths ranged from 0.01 to 0.09 kg m<sup>-2</sup> for the six cases presented. The SSM/I algorithms investigated predicted LWP to within  $\pm 0.02$ –0.03 kg m<sup>-2</sup>, provided one accounted for systematic biases in the retrievals. These biases were systematic in the range  $\pm 0.06$  kg m<sup>-2</sup> and were presumably caused by latitudinal and seasonal influences inherent in the algorithms. Algorithms based on radiative transfer models appeared to perform better than the statistically based algorithms.

### 1. Introduction

Considerable current research has focused on the usefulness of satellite-based microwave measurements in determining geophysical fields, especially over the oceans where ground-based measurements are scarce. In particular, the Defense Meteorological Satellite Program Special Sensor Microwave/Imager (DMSP SSM/I) (Hollinger et al. 1990) has been used to determine sea surface winds (Goodberlet et al. 1989, 1990), total precipitable water (Alishouse et al. 1990a; Petty 1990; Greenwald et al. 1993), and integrated cloud liquid water path (Alishouse et al. 1990b; Petty 1990; Liu and Curry 1993; Greenwald et al. 1993). These algorithms all rely on brightness temperatures from some or all of the SSM/I 19-, 22-, 37-, and 85-GHz channels. Although algorithms for sea surface winds can be calibrated by use of buoys, and total precipitable water can be calibrated by use of upsondes, the calibration of integrated cloud liquid water path (LWP) has been hampered by a lack of in situ data and has relied on correlations with either ground-based microwave radiometers or output from radiative transfer models.

Intercomparisons between LWP algorithms have shown significant differences (Liu and Curry 1993; Greenwald et al. 1993; Prigent et al. 1994). Disagreements have been attributed to simplistic natures of the

radiative transfer models, the lack of in situ data for determining parameterizations, biases in the parameterizations caused by seasonal or latitudinal influences, errors associated with failure to uncouple total precipitable water from integrated cloud liquid water, and poor knowledge of cloud temperature. Each study has pointed to the lack of in situ measurements as a limitation in the verification of the algorithms. Although measurements from research aircraft that are simultaneous with a satellite overpass are quite scarce (Petty and Katsaros 1992), they might provide a valuable validation technique for the LWP retrieval algorithms.

The Second Canadian Atlantic Storms Program (CASP II) was conducted by the Atmospheric Environment Service and Institute of Aerospace Research of Canada. It was based out of St. John's, Newfoundland, and was conducted between 15 January 1992 and 15 March 1992. Although the primary objective of the project was to investigate the mesoscale structure of East Coast winter storms (Stewart 1991), there was an aircraft-icing research component (Cober et al. 1995; Patnoe et al. 1993), part of which was designed to examine the usefulness of satellite-based microwave measurements in determining regions of potentially dangerous aircraft icing over the ocean. Curry and Liu (1992) and Lee et al. (1994) have suggested the use of satellite data for this purpose. Several CASP II flights were conducted under *F-10* and *F-11* SSM/I satellite overpasses to perform an intercomparison between LWP measured from the aircraft and LWP inferred from several algorithms. Comparisons between aircraft and satellite data for six CASP II flights are reported here. Although the results do not allow for a

---

*Corresponding author address:* Dr. Stewart G. Cober, Cloud Physics Research Division ARMP, Atmospheric Environment Service, 4905 Dufferin Street, Downsview, ON M3H 5T4, Canada.

TABLE 1. Summary of the SSM/I geophysical algorithms used in the analysis. Column 1 includes an abbreviated name for each algorithm. The channels required for each algorithm, as well as other specific input parameters, are listed. Here  $T_c$  is the cloud-top or mean cloud temperature,  $T_s$  the surface temperature, and  $T_a$  the mean atmospheric temperature.

SSM/I algorithm	19H	19V	22V	37H	37V	85H	85V	Other input
SWS Goodberlet								
Goodberlet et al. (1989)		×	×	×	×			
SWS modified Petty								
Colton and Poe (1994)		×	×	×	×			TPW
TPW Petty								
Petty (1990)	×	×	×					
TPW modified Petty								
Colton and Poe (1994)		×	×	×				
TPW Alishouse								
Alishouse et al. (1990a)		×	×		×			nonlinear 22V
TPW Greenwald								
Greenwald et al. (1994)	×	×		×	×			$T_c$ , $T_s$ , SWS, LWP
LWP Petty								
Petty (1990)				×	×			SWS, TPW
LWP modified Petty								
Colton and Poe (1994)				×	×			$T_c$ , SWS, TPW
LWP Alishouse 6								
Hollinger (1991)	×	×	×	×	×	×		
LWP Alishouse 4h								
Alishouse et al. (1990b)	×		×		×	×		
LWP Alishouse 4l								
Hollinger (1991)	×		×	×	×			
LWP Alishouse 1								
Hollinger (1991)					×			
LWP Liu and Curry 37H								
Liu and Curry (1993)				×				$T_c$ , $T_s$ , $T_a$
LWP Liu and Curry 37V								
Liu and Curry (1993)					×			$T_c$ , $T_s$ , $T_a$
LWP Greenwald								
Greenwald et al. (1993)	×	×		×	×			$T_c$ , $T_s$ , SWS, TPW

detailed statistical analysis and are biased in terms of representing limited latitude and seasonal variations, they do provide insight into the accuracy of several SSM/I algorithms under different meteorological situations.

## 2. SSM/I retrieval algorithms

Summaries of geophysical field retrievals, as inferred from satellite microwave measurements, have been given by Greenwald et al. (1993) and Liu and Curry (1993). Summaries of SSM/I retrieval algorithms have been given by Hollinger (1991) and Colton and Poe (1994). The LWP algorithms from Alishouse et al. (1990b), Petty (1990), Liu and Curry (1993), and Greenwald et al. (1993) were chosen for comparison with the aircraft data, and a brief overview of each is discussed below. Because surface wind speed (SWS) and total precipitable water (TPW) algorithms are often coupled with LWP algorithms, these retrieval algorithms were also included in the comparisons. A summary of the SSM/I channels required for each algorithm is given in Table 1. SSM/I channels are referred to as 19H, 19V, 22V, 37H, 37V, 85H, and 85V,

where the numbers represent the channel frequencies in gigahertz and H and V refer to horizontal or vertical polarizations, respectively. SSM/I retrievals presented here were derived from quality-controlled antenna brightness temperatures purchased from Remote Sensing Systems, Inc.

Alishouse et al. (1990b) presented a global algorithm where ground-based microwave radiometer measurements from San Nicolas Island and Kwajalein Island were compared with linear fits of the SSM/I brightness temperatures from four channels (Table 1). The best fit was based on only 20 data points and was not considered verified for LWPs close to zero. This algorithm has been criticized by Liu and Curry (1993) as saturating for LWPs larger than  $1 \text{ kg m}^{-2}$  and as possibly not being representative for latitudes and seasons outside those from where the ground validation measurements were taken. Greenwald et al. (1993) have shown that the algorithm tends to underestimate LWP by up to a factor of 2, presumably because it failed to uncouple TPW (mainly water vapor) from LWP (cloud water). This limitation has also been noted by Petty (1990), who stated that the LWP calculations of Alishouse et al. (1990b) were highly cor-

related with TPW. Prigent et al. (1994) have criticized the algorithm as not being statistically different from zero. However, their reasoning was incorrect because they assumed that the algorithm had an accuracy of  $0.4 \text{ kg m}^{-2}$ , which was larger than the value of most of the 20 data points used in the original fit. In fact, Alishouse et al. (1990b) stated that the accuracy was less than  $0.04 \text{ kg m}^{-2}$  and that the algorithm was expected to be most accurate for LWP around  $0.14 \text{ kg m}^{-2}$ . Regardless of the criticisms, the Alishouse et al. (1990b) algorithm is the only one that has been validated by direct 1:1 comparisons with ground-based LWP measurements. Four separate LWP algorithms, hereafter referred to as the Alishouse 6, 4h, 4l, and 1 channel algorithms, which use 6, 4, and 1 SSM/I channels, respectively (Table 1), have been detailed in Hollinger (1991). The 4h algorithm uses 85-GHz data, while the 4l algorithm does not. An algorithm for TPW was given by Alishouse et al. (1990a) and will be referred to as the Alishouse TPW algorithm.

Petty (1990) developed a set of equations for the determination of SWS, TPW, and LWP based on SSM/I brightness temperatures. He used the statistical SWS algorithm of Goodberlet et al. (1989) and smoothed the wind field by averaging over a  $3 \times 3$  pixel area. Petty developed two LWP algorithms that used the 37- and 85-GHz data, respectively, and showed that the minimum rms error for zero LWP (clear sky) cases was about  $0.025 \text{ kg m}^{-2}$ . Liu and Curry (1993) found that the Petty algorithms tended to work poorly in the Tropics but agreed with their own in other areas for nonprecipitating clouds. Greenwald et al. (1993) found that the 37-GHz Petty algorithm compared well with their own, although it tended to show larger disagreement at small LWP values ( $<0.1 \text{ kg m}^{-2}$ ). The 37-GHz algorithm is used in the comparisons described here and will be referred to as the Petty algorithm. Similarly, the SWS algorithm of Goodberlet et al. (1989) will be referred to as the Goodberlet algorithm. Modified algorithms for SWS, TPW, and LWP have been reported by Petty in the 1993 DMSP SSM/I Algorithm Symposium (Colton and Poe 1994). These algorithms were believed to be less susceptible to correlations between LWP and TPW and will be referred to here as the modified Petty algorithms. Another difference in the modified LWP algorithm was the inclusion of the cloud temperature in the calculation of LWP.

Liu and Curry (1993) developed a LWP algorithm based on a 32-stream plane-parallel radiative transfer model with both ice and water phases and precipitating and nonprecipitating clouds. They indirectly verified their algorithm by showing that the average LWP for clear skies was effectively zero, although they did not discuss the standard error around zero for clear-sky cases. The algorithm was examined for regions in the tropical Pacific Ocean, North Atlantic Ocean, and western Pacific Ocean. Comparisons of their algorithm were made with those of Petty

(1990), Alishouse et al. (1990b), and Greenwald et al. (1993), and they concluded that it seemed to work well in clear-sky cases, cases with liquid and mixed-phase clouds, and cases with precipitating clouds. Although their algorithm could be used to determine LWP using any one of the 19- or 37-GHz vertically or horizontally polarized channels, they preferred the 37H channel for determining LWP from nonprecipitating clouds.

Greenwald et al. (1993) developed a plane-parallel radiative transfer model that allowed LWP and TPW to be inferred from the 19- and 37-GHz channels of the SSM/I. Their model was based on a nonprecipitating single cloud layer. They validated their algorithm by performing an extensive comparison with ground-based microwave radiometer measurements from locations in the North Sea, western Pacific, and off the California coast and showed that the minimum rms error for clear-sky cases was  $0.016 \text{ kg m}^{-2}$ . They concluded that reasonably accurate measurements of LWP could be derived from SSM/I observations of nonprecipitating cloud systems, particularly in areas of persistent stratocumulus clouds. They also applied their algorithm to determine the average cloud liquid water path over the oceans. This algorithm was criticized by Liu and Curry as not being applicable to precipitating clouds or systems in which more than one layer existed. Liu and Curry (1993) found that the Greenwald et al. (1993) algorithm gave results close to their own, provided that a realistic cloud temperature was used. This algorithm will be referred to as the Greenwald algorithm.

### 3. Aircraft and instrumentation

The primary research aircraft used during CASP II was a Convair-580, which was fully instrumented for cloud microphysics measurements. Table 2 summarizes the onboard instrumentation applicable to this investigation. A summary of the calibrations, errors, and limitations of these instruments is detailed in Cober et al. (1995), although a brief summary will be discussed below.

Liquid water content (LWC) was measured by two Particle Measuring Systems (PMS) King probes to within  $\pm 15\%$ , while temperature was measured to within  $1^\circ\text{C}$  by two Rosemount temperature probes and a reverse flow temperature probe. Dewpoint was measured by a Cambridge dewpoint hydrometer to  $\pm 1^\circ\text{C}$ . Latitude and longitude were measured with GPS, INS, and Loran navigation systems and were considered accurate to within 5 km. The instruments used during the project were well calibrated, with extensive quality control analysis performed on the data (Cober et al. 1995).

Ice crystals were measured with three Particle Measuring Systems 2D probes (Table 2). Ice crystal con-

TABLE 2. Summary of instruments mounted on the Convair-580 during CASP II that were applicable to this investigation. PMS indicates instruments made by Particle Measuring Systems.

Instrument	Notes
PMS King probe	Short-wire version
PMS King probe	Long-wire version
	Range selections to
PMS FSSP 100× extended range	5–95 $\mu\text{m}$
PMS 2DC mono	25–800 $\mu\text{m}$
PMS 2DC gray	25–1600 $\mu\text{m}$
PMS 2DP mono	200–6400 $\mu\text{m}$
Pitot static pressure tubes	two sensors
Rosemount 858 gust probe	
Cambridge dewpoint hygrometer	
Rosemount temperature sensor	two sensors
Reverse flow temperature sensor	
GPS, INS, Loran navigation systems	
Lightweight Loran Digital	
Dropsonde system	

concentrations reported in this paper refer to combinations of measurements from all three probes and reflect concentrations for ice crystals between 0.1 and 6.4 mm in size. Crystals smaller than 100  $\mu\text{m}$  are not included in the concentrations because of large depth of field errors in the first two to four channels of the three 2D probes. The aircraft-based LWC and LWP measurements reported here do not include contributions from ice particles.

On some flights a Lightweight Loran Digital Dropsonde (L2D2) system developed by NCAR was employed to provide additional information about the atmosphere below the aircraft. These soundings were useful for verifying cloud top altitude, cloud temperature, and surface wind speeds. Dropsonde measurements had the following accuracy and ranges: pressure  $\pm 0.2$  kPa between 20 and 105 kPa; temperature  $\pm 0.5^\circ\text{C}$  between  $-55^\circ$  and  $40^\circ\text{C}$ ; humidity  $\pm 5\%$ – $13\%$  between 5% and 100%, depending on temperature; and wind speed  $\pm 1$   $\text{m s}^{-1}$ . Dropsondes also provided useful measurements of the TPW below the aircraft.

#### 4. Comparison methodology

The majority of the LWP retrieval algorithms rely mainly on measurements from the SSM/I 37-GHz channel. This channel has a pixel size of approximately 28 km  $\times$  37 km, with satellite retrievals of LWP representing an average over a volume. Assuming a single-layer cloud with a thickness of 1 km, a satellite-derived LWP from a single pixel would represent 700  $\text{km}^3$  of cloud. Conversely, aircraft measurements were 1-s averages, representing 100-m segments through a cloud. A 5-min average would represent 30 km, which is similar to the length of the 37-GHz SSM/I pixel. Consequently, aircraft measurements of LWC taken during several 5-min passes, each at a different altitude in the same cloud, would allow characterization of the cloud

LWC along a horizontal–vertical plane on the scale of an SSM/I pixel. Assuming the cloud was relatively homogeneous over a 30 km  $\times$  30 km area, the LWC profile measured by the aircraft along the horizontal–vertical plane should be representative of the cloud volume through which the horizontal–vertical plane intersects. This was the methodology behind the comparison between the aircraft and satellite measurements.

The aircraft measurements were generally along a straight flight track between 50 and 200 km in length. These gave good horizontal characterizations of the cloud on the scale of several SSM/I pixels. Multiple passes at different altitudes and vertical profiles were performed to ensure sufficient vertical characterization of the clouds. Data over a 25-km flight segment was rarely sufficient to characterize the cloud and allow a direct comparison between aircraft and satellite measurements for a single and coincident SSM/I pixel. For example, a 25-km flight segment might have only had aircraft data across two altitudes and no vertical profiles, while a 100-km segment may have had data at four altitudes and two full vertical profiles. This would allow more confidence in the 100-km characterization than in the 25-km characterization, although it would require that the assumption of homogeneous clouds be valid over a correspondingly larger region. Obviously, the LWP derived from satellite measurements would need to be averaged over all pixels that the aircraft crossed in the 100-km flight track. This actually eases the aircraft–satellite comparison because it reduces the problem of determining aircraft satellite spacial coincidence on 25-km scales, which can be difficult given the errors in aircraft navigation and satellite geolocation. Averages of SSM/I data over several pixels also reduce the errors caused by radiometer noise.

The most important assumption with this technique is that the clouds are relatively homogeneous over the area being averaged. The variability of the aircraft and SSM/I measurements are potential indicators of the validity of this assumption. Homogeneous clouds in the unmeasured plane were assumed if satellite photographs showed wide regions of stratus clouds that appeared unchanged over several hours.

For each flight, all 1-s LWC measurements were averaged into altitude bins of 100 m. The LWP was calculated by integrating the average LWCs over all altitude bins from cloud base to cloud top. Errors in aircraft-derived LWP were based on integrating the LWC variability (standard deviation) over all altitude bins. There was no difference in the LWP calculations using altitude bins of 10 or 400 m. The standard deviation of LWC for a single-altitude bin was a measure of the horizontal variability of the cloud at that altitude. The errors listed for LWP measurements derived from SSM/I data are the standard deviations of average values taken over several pixels and physically represent the horizontal variability of the SSM/I measurements. Such errors were sometimes smaller than the estimated

accuracy of the algorithms, which ranged from  $0.04 \text{ kg m}^{-2}$  for the Alishouse algorithms to  $0.02 \text{ kg m}^{-2}$  for the Greenwald algorithm (section 2). Account will be taken of the estimated retrieval accuracies in section 6.

## 5. Case studies

### a. General

Case studies were selected if several conditions were met. The aircraft had to be flying over the ocean and not over a region of sea ice. There had to be a simultaneous or near-simultaneous SSM/I overpass (within 2 h, providing the clouds were unchanging). Finally, the aircraft had to make several horizontal passes at different altitudes and one or more vertical profiles from cloud base to cloud top. This ensured that the LWC profile of the cloud along a horizontal-vertical plane was a sufficient characterization of the cloud. There were six flights that met these criteria. On two of these flights, the clouds were continuous single-layered stratus decks, while on three flights the clouds were broken single-layered stratus decks (streamers), with between 40% and 75% surface coverage. On the remaining flight, the clouds were also stratus, although, were deeper and were associated with a warm frontal region. In all cases, the clouds were considerably greater than 30 km in horizontal extent. Each case will be discussed separately to substantiate the comparison of aircraft data with SSM/I measurements. LWPs for these six cases varied from  $0.006$  to  $0.09 \text{ kg m}^{-2}$ . As a comparison, the average LWP for clouds over the North Atlantic Ocean was found by Curry et al. (1990) to be  $0.1 \text{ kg m}^{-2}$ , while Greenwald et al. (1993) found the global average LWP for nonprecipitating clouds to be  $0.08 \text{ kg m}^{-2}$ .

### b. Case 1, 10 March 1992: Solid, nonglaci-ated, stratiform clouds

Low solid stratus clouds formed between Nova Scotia and Newfoundland on 10 March 1992. Winds near the surface were very light, and the cloud persisted for several hours. A flight was conducted to coincide with the 2006 UTC *F-11* SSM/I overpass. Figure 1 shows the 1847 UTC *NOAA-11* visible image, with the aircraft flight track between 2040 and 2200 UTC superimposed. The aircraft flew several passes along the indicated track, which was approximately 175 km in length, although only the east portion of the flight track (about 70 km) was over the open ocean, with the remainder being over sea ice. The sea ice was determined from SSM/I sea ice algorithms from Hollinger (1991). The cloud was capped by a strong inversion, with a cloud-top temperature of  $-6^{\circ}\text{C}$  and with concentrations of ice crystals of less than  $1 \text{ L}^{-1}$ . *NOAA* satellite images at  $11 \mu\text{m}$  showed that within the resolution of the satellite (approximately 1 km) the cloud was continu-

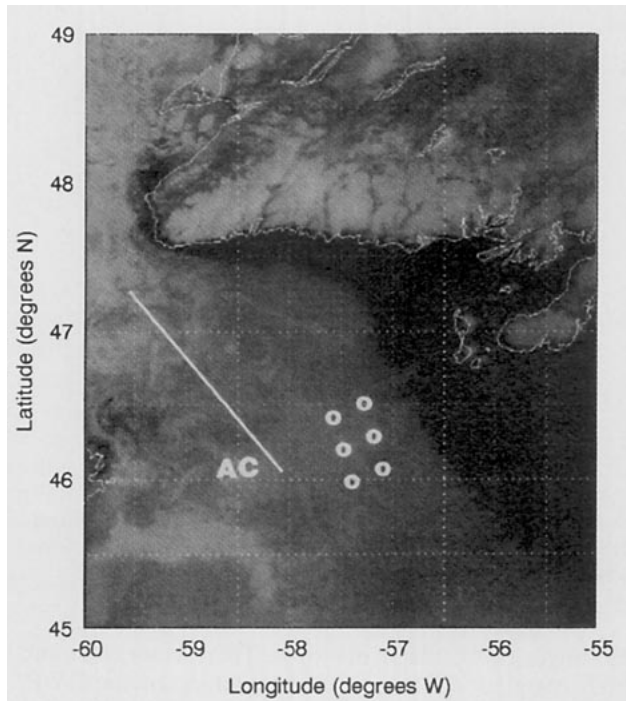


FIG. 1. *NOAA-11* 1847 UTC 10 March 1992 visible satellite image. The centers of the 37-GHz SSM/I pixels used for the comparison with aircraft data are indicated with white circles. The aircraft flight track is labeled AC.

ous and had a cloud-top temperature of  $-7^{\circ}\text{C}$ , with less than  $1^{\circ}\text{C}$  of variability along the flight track.

Cloud-top height varied between 280 and 325 m and was lowest toward the west edge of the flight track. There was no obvious observed difference in the clouds measured over the sea ice and over the ocean. Figure 2 shows the variation of LWC with altitude for a period in which the aircraft performed a vertical profile through the cloud (2150–2200 UTC). The liquid profile content was highly stratified with altitude and was equal to about 0.6 of the adiabatic value, assuming that the cloud extended to the ocean surface. The aircraft did not fly below cloud base, with the lowest altitude reached being 84 m. For the cloud profile shown in Fig. 2, the LWP was  $0.042 \text{ kg m}^{-2}$ , of which the extrapolated contribution from the cloud below 84 m was  $0.0015 \text{ kg m}^{-2}$ .

The aircraft-measured cloud-top LWC averaged for seven 25-km intervals varied between 0.23 and  $0.35 \text{ g m}^{-3}$ . For similar LWC profiles to Fig. 2, these implied LWPs from  $0.032 \pm 0.005$  to  $0.057 \pm 0.010 \text{ kg m}^{-2}$ . The average in situ LWP for all seven segments was  $0.043 \pm 0.011 \text{ kg m}^{-2}$ , where the error represents the standard deviation of the seven measurements.

The LWP retrievals from the Alishouse six-channel algorithm are shown in Fig. 3 (other algorithms showed similar results). Each point represents the center of a 37-GHz pixel. The sea ice edge ( $>5\%$  coverage) from

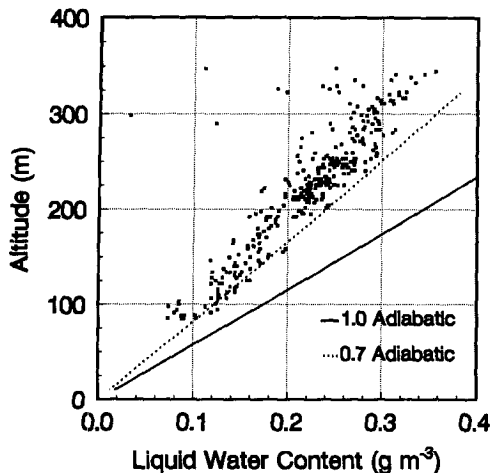


FIG. 2. Vertical profile of LWC measured with the aircraft between 2150 and 2200 UTC 10 March 1992. Data points represent 1-s averages. The curves represent fractional adiabatic profiles.

Hollinger (1991) is also shown. There is an apparent high correlation between the magnitude of the LWP and the location of the ice edge, with significantly overestimated values of LWP near and over the sea ice. Since the 19-GHz channel has a resolution of 50–70 km, it was expected to see contaminated LWP values up to two pixels (37 GHz) from the ice edge, since most LWP algorithms rely on 19-GHz data. Unfortunately, the aircraft flight track over the open ocean was within two pixels of the sea ice, so that no direct comparisons with SSM/I pixels were possible. However, the cloud was homogeneous, as measured from the aircraft during the 175-km flight track and as observed with several NOAA satellite images. Therefore, the aircraft measurements were compared to the SSM/I pixels just east of the flight track, which were outside of the ice-edge contamination region but were within the same cloud, at the same latitude, and within 100 km of the flight track. There were six SSM/I pixels (Figs. 1 and 3) for which geophysical fields were compared to the aircraft data.

Comparisons between surface and aircraft measurements and the SSM/I-retrieved fields are given in Table 3. The errors listed for the SSM/I measurements represent the standard deviation of mean values from the six pixels. In general, the aircraft and satellite measurements agreed within the measurement errors. For example, the aircraft LWP was  $0.043 \pm 0.011 \text{ kg m}^{-2}$ , while the Alishouse six-channel LWP was  $0.032 \pm 0.010 \text{ kg m}^{-2}$ . Detailed comparisons between aircraft and SSM/I measurements will be discussed in section 6.

### c. Case 2, 4 March 1992: Solid, partly glaciated, stratiform clouds

A wide band of persistent stratiform cloud formed over the Gulf Stream, near 40°N, 50°W, on 4 March

1992. Figure 4 shows the 1818 UTC NOAA-11 satellite image. A flight was conducted to coincide with the 1944 UTC SSM/I F-11 satellite overpass, and the flight track between 1920 and 2020 UTC is shown in Fig. 4. The in-cloud flight track was 80 km and included several horizontal and vertical passes. Cloud top was 3100 m, while the lowest altitude that the aircraft flew in the cloud region was 900 m. Cloud base was estimated at 700 m by extrapolating the LWC values between 900 and 1200 m along an adiabatic profile. The cloud-top temperature was  $-15^{\circ}\text{C}$ , with ice crystal concentrations varying from 20 to  $50 \text{ L}^{-1}$  throughout, although the glaciation was greater in the upper portions of the cloud. The ice crystal size distribution was exponential; with crystals with diameters greater than 1 mm having maximum concentrations of  $3 \text{ L}^{-1}$ . The regions of supercooled liquid water content (SLWC) were patchy, being broken by regions of glaciated cloud. Patches of SLWC averaged  $2.2 \pm 2.1 \text{ km}$  in length, where the error represents the standard deviation. Maximum SLWCs on a 2-km scale were  $0.2 \text{ g m}^{-3}$ , with maximum 1-s peaks of  $0.5 \text{ g m}^{-3}$ . The liquid water content variation with altitude throughout this region is shown in Fig. 5. The LWC only approached the adiabatic value for regions low in the cloud, and the peak LWC values between 900 and 1200 m were consistent with a cloud base of 700 m.

As discussed in section 4, the LWC was averaged into altitude intervals of 100 m for all data accumulated from the 80-km flight track. The average liquid water contents at each altitude ranged from 0.01 to  $0.06 \text{ g m}^{-3}$ , which are unrepresentative of the regions of

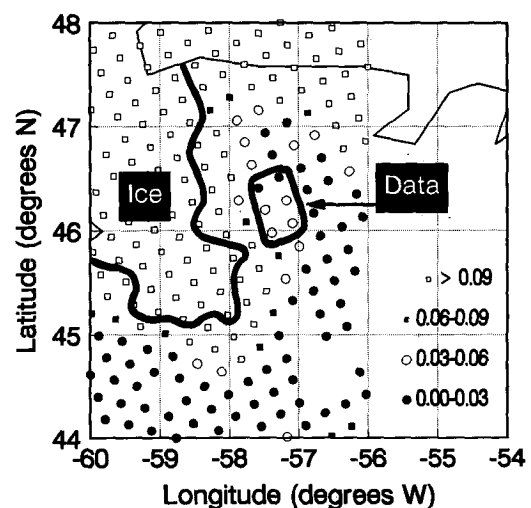


FIG. 3. SSM/I measurements of LWP ( $\text{kg m}^{-2}$ ) from the Alishouse six-channel algorithm for 10 March 1992. Each point represents the centre of a 37-GHz pixel. The pixels used for the comparison with aircraft data are labeled Data. Regions with greater than 5% sea-ice coverage, as based on Hollinger (1991), are labeled Ice. Only data from pixels covering  $4^{\circ}$  longitude by  $4^{\circ}$  latitude are shown.

TABLE 3. Summary of aircraft- and SSM/I-measured geophysical fields for each of the six case studies. Units for SWS, TPW, and LWP are meters per second, kilograms per square meter, and kilograms per square meter, respectively. Terms AC, SB, and DS refer to measurements from aircraft instruments, surface buoys, and dropsondes, respectively.

Algorithm	Case 1	Case 2	Case 3
SWS measured	0–2.5 (6SB)	10.8 (2DS)	7–10 (3SB)
SWS	$2.3 \pm 1.0$	$12.3 \pm 1.5$	$9.0 \pm 1.4$
SWS Petty (mod)	$1.5 \pm 0.8$	$11.7 \pm 1.6$	$8.0 \pm 1.4$
TPW measured	6.9 (2AC)	7.4 (DS/AC)	5.9 (2DS)
TPW Petty	$7.8 \pm 0.5$	$8.6 \pm 0.5$	$6.9 \pm 0.5$
TPW Petty (mod)	$6.0 \pm 0.8$	$8.2 \pm 0.5$	$5.7 \pm 0.4$
TPW Alishouse	$6.0 \pm 0.6$	$7.9 \pm 0.5$	$7.0 \pm 0.3$
TPW Greenwald	$11.1 \pm 1.1$	$12.9 \pm 0.6$	$11.3 \pm 0.4$
LWP measured	$0.043 \pm 0.011$	$0.064 \pm 0.017$	$0.0065 \pm 0.0041$
LWP Petty	$0.076 \pm 0.013$	$0.152 \pm 0.038$	$0.060 \pm 0.016$
LWP Petty (mod)	$0.055 \pm 0.007$	$0.098 \pm 0.023$	$0.045 \pm 0.009$
LWP Alishouse 6	$0.035 \pm 0.010$	$0.088 \pm 0.024$	$0.013 \pm 0.005$
LWP Alishouse 4h	$0.032 \pm 0.010$	$0.087 \pm 0.024$	$0.016 \pm 0.006$
LWP Alishouse 4l	$0.020 \pm 0.013$	$0.076 \pm 0.024$	$-0.009 \pm 0.007$
LWP Alishouse 1	$-0.017 \pm 0.008$	$0.038 \pm 0.019$	$-0.044 \pm 0.004$
LWP Liu 37H	$0.004 \pm 0.009$	$0.089 \pm 0.027$	$-0.006 \pm 0.007$
LWP Liu 37V	$0.016 \pm 0.008$	$0.064 \pm 0.022$	$-0.014 \pm 0.005$
LWP Greenwald	$0.034 \pm 0.009$	$0.071 \pm 0.017$	$0.010 \pm 0.009$

Algorithm	Case 4	Case 5	Case 6
SWS measured	10–13 (2SB)	21–25 (2SB)	14.5 (DS)
SWS	$11.6 \pm 1.0$	$26.4 \pm 0.8$	$14.5 \pm 1.2$
SWS Petty (mod)	$10.3 \pm 1.0$	$25.1 \pm 0.8$	$14.4 \pm 1.2$
TPW measured	4.7	2.3 (AC)	11.8 (AC/DS)
TPW Petty	$5.3 \pm 0.3$	$1.9 \pm 0.4$	$10.9 \pm 0.3$
TPW Petty (mod)	$4.1 \pm 0.2$	$4.2 \pm 0.3$	$11.7 \pm 0.5$
TPW Alishouse	$5.9 \pm 0.3$	$5.5 \pm 0.3$	$11.6 \pm 0.7$
TPW Greenwald	$8.7 \pm 0.4$	$8.5 \pm 0.5$	$15.8 \pm 1.0$
LWP measured	$0.010 \pm 0.006$	$0.032 \pm 0.009$	$0.09 \pm 0.02$
LWP Petty	$0.072 \pm 0.015$	$0.202 \pm 0.006$	$0.37 \pm 0.06$
LWP Petty (mod)	$0.054 \pm 0.009$	$0.085 \pm 0.005$	$0.25 \pm 0.05$
LWP Alishouse 6	$0.027 \pm 0.008$	$0.199 \pm 0.008$	$0.18 \pm 0.02$
LWP Alishouse 4h	$0.030 \pm 0.008$	$0.206 \pm 0.008$	$0.19 \pm 0.02$
LWP Alishouse 4l	$-0.001 \pm 0.009$	$0.143 \pm 0.008$	$0.15 \pm 0.02$
LWP Alishouse 1	$-0.047 \pm 0.004$	$0.021 \pm 0.003$	$0.11 \pm 0.02$
LWP Liu 37H	$0.005 \pm 0.009$	$0.008 \pm 0.009$	$0.12 \pm 0.05$
LWP Liu 37V	$-0.008 \pm 0.004$	$0.009 \pm 0.003$	$0.14 \pm 0.05$
LWP Greenwald	$0.010 \pm 0.007$	$0.017 \pm 0.005$	$0.16 \pm 0.04$

sustained LWC and reflect the degree of glaciation of the cloud. Integration of the average LWCs with altitude was used to calculate the LWP. The aircraft made approximately four passes at different altitudes during the 60-min period of interest, and the average LWC measurements provide a good characterization of the cloud along the entire flight track. The average LWP for the aircraft was  $0.064 \pm 0.017 \text{ kg m}^{-2}$ , of which  $0.002 \text{ kg m}^{-2}$  was the extrapolated contribution from the cloud below 900 m.

The SSM/I LWP retrievals from the Liu and Curry 37V algorithm are shown in Fig. 6. SSM/I pixels to the northwest had retrieved LWPs of less than  $0.0 \text{ kg m}^{-2}$ , while pixels south of  $41^\circ\text{N}$  were identified as having possible precipitation by the Goodberlet algorithm. The latter clouds were likely more convective than the clouds flown through during the flight and may have been precipitating. There were seven SSM/I pix-

els (Figs. 4 and 6) that the flight path crossed for which the SSM/I-retrieved geophysical fields were averaged. None of the seven pixels were within a precipitation region using the classifications of Alishouse, Goodberlet, or Petty. The Liu and Curry 37V algorithm appears to have defined the northern cloud boundary fairly well and shows the LWP increasing to the southeast. The aircraft flight track was oriented along the gradient of LWP, so that the aircraft measurements will incorporate this nonhomogeneity of the cloud field. The aircraft and satellite LWP values agreed within the variability of the measurements (Table 3). The variability for both the aircraft and SSM/I LWP measurements was approximately  $0.02 \text{ kg m}^{-2}$ , which is small enough to support the assumption of homogeneous clouds in the region of the flight.

There was sufficient vertical aircraft data along a single 25-km segment to allow a direct comparison with

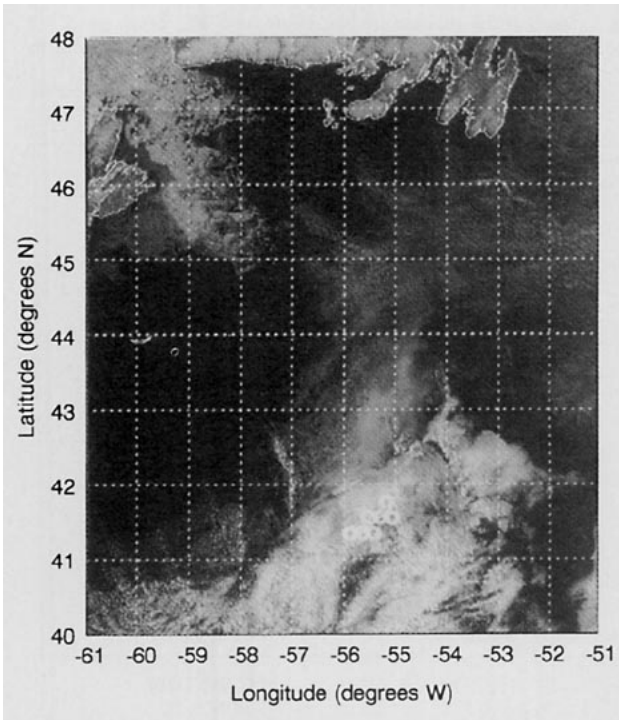


FIG. 4. NOAA-11 1818 UTC 4 March 1992 visible satellite image. Markings are as in Fig. 1. The portion of the aircraft trajectory used in the comparison with SSM/I data is indicated by the straight white line that overlaps the SSM/I markings.

an SSM/I pixel. The LWP for the aircraft was  $0.076 \pm 0.010 \text{ kg m}^{-2}$ , while the Alishouse 6, Liu and Curry 37H, and Greenwald algorithms gave 0.072, 0.094, and  $0.064 \text{ kg m}^{-2}$ , respectively. The agreement between the algorithms and aircraft data further illustrates that the comparison technique between the aircraft and SSM/I data is reasonable for this case.

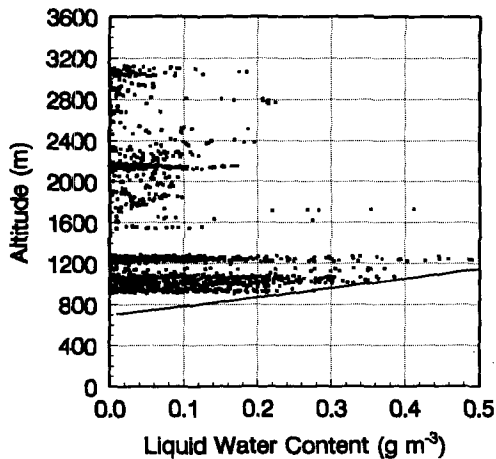


FIG. 5. Vertical profile of LWC measured with the aircraft between 1920 and 2020 UTC 4 March 1992. The solid curve represents an adiabatic LWC profile for the lower cloud.

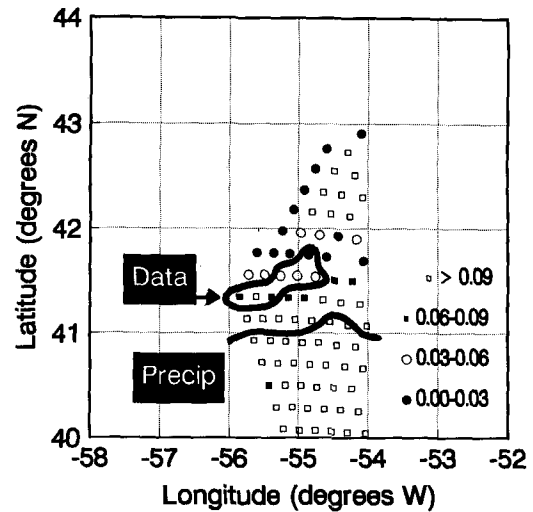


FIG. 6. SSM/I measurements of LWP ( $\text{kg m}^{-2}$ ) from the Liu and Curry 37V algorithm for 4 March 1992. Markings are as in Fig. 3. Pixels in which precipitation was indicated by the Goodberlet algorithm are labeled "Precip". The southwest boundary of the SSM/I data represents the edge of the satellite swath. SSM/I pixels to the northwest have retrieved LWPs less than  $0.0 \text{ kg m}^{-2}$ . Only data points west of  $54^\circ\text{W}$  are shown.

*d. Case 3, 11 February 1992: Thin streamer clouds*

Figure 7 shows streamer clouds that formed southeast of Newfoundland on 11 February 1992. A research

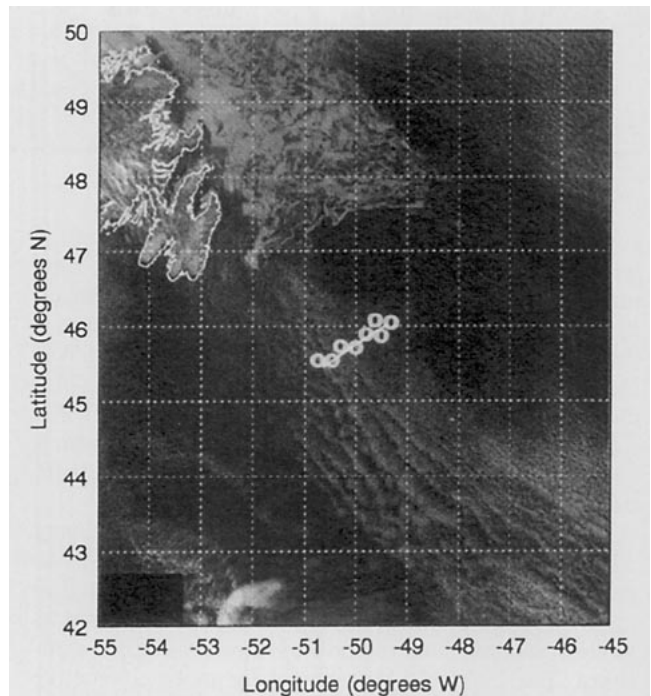


FIG. 7. NOAA-12 1739 UTC 11 February 1992 visible satellite image. Markings are as in Fig. 1.

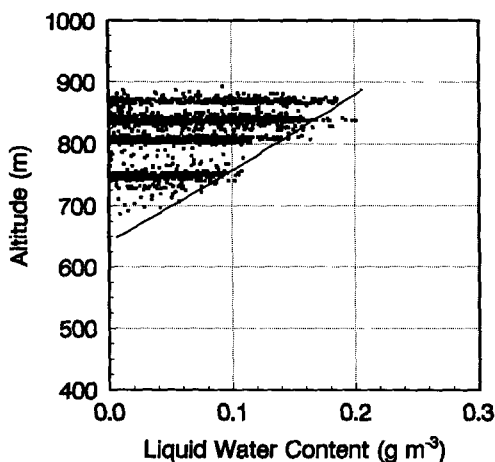


FIG. 8. Vertical profile of LWC measured with the aircraft between 1930 and 2050 UTC 11 February 1992. Markings are as in Fig. 5.

flight was conducted into the streamer cloud region to coincide with the 1918 UTC SSM/I *F-11* overpass. The aircraft flew in the cloud region from 1930 to 2050 UTC, performing two passes with several vertical profiles along the 112-km flight track shown in Fig. 7. Satellite images showed that the cloud fields were unchanged over the period of the flight. A low-level inversion at  $-11^{\circ}\text{C}$  capped a thin saturated layer where the streamer clouds formed. The clouds were supercooled with ice crystal concentrations between 0.3 and  $1.1\text{ L}^{-1}$ . The clouds were broken, with the aircraft being in cloud 47% of the time while crossing the cloud region in a direction perpendicular to the orientation of the streamers. Patches of SLWC were an average of  $2.3 \pm 1.9\text{ km}$  in length. This is smaller than the size of the streamers, which varied between approximately 5 and 10 km across, as estimated from NOAA IR and visible images. In-cloud SLWCs averaged  $0.08 \pm 0.03\text{ g m}^{-3}$ , with the maximum 1-s SLWC measured being  $0.2\text{ g m}^{-3}$ . The liquid water content profile with altitude is shown in Fig. 8. The cloud was 230 m thick, with peak LWCs at all altitudes reaching the adiabatic values. Since the flight track crossed the streamers perpendicular to their orientation and was long enough to include measurements from several streamer clouds, the average aircraft measurements were a good characterization of the clouds in the region of the flight and were not biased by excessive measurements in clear air (i.e., between the streamers) or in a single streamer cloud. Figure 8 shows that there was sufficient LWC data at all altitudes to allow a good characterization of the cloud field.

The aircraft LWP averaged across the flight track shown in Fig. 7 was  $0.0065 \pm 0.0041\text{ kg m}^{-2}$ , where the error is representative of the horizontal variability of liquid water content. The average aircraft measurement was compared to the eight SSM/I pixels covering

the flight track (Fig. 7). Given that LWP algorithms have accuracies of  $0.02\text{--}0.03\text{ kg m}^{-2}$  (see section 2) for no-cloud (clear sky) cases, they may not be able to distinguish a LWP of  $0.01\text{ kg m}^{-2}$  from a clear sky. Regardless, the aircraft and SSM/I LWP measurements agreed within  $0.01\text{--}0.02\text{ kg m}^{-2}$  (Table 3).

*e. Case 4, 15 February 1992: Partially glaciated streamer clouds*

This was a similar case to 11 February 1992 (case 3), although the clouds were more developed and more glaciated. Streamer clouds formed east of St. John's and persisted for several hours. Figure 9 shows the 1830 UTC NOAA-12 satellite photo taken just prior to the research flight. The flight was conducted to make LWP measurements to compare with the *F-11* 2009 UTC and *F-10* 2320 UTC satellite overpasses. Aircraft measurements were made between 2100 and 2300 UTC and, given the persistent nature of the clouds, should allow for a good comparison with data from both satellite overpasses. The streamers were broken with the aircraft being in cloud 40% of the time during flight through the cloud region. The aircraft trajectory was at an angle of about  $45^{\circ}$  to the streamer orientation, so that the aircraft crossed several different streamer clouds during the flight. The flight west of  $50^{\circ}\text{W}$  was over or near the sea ice, while the flight east of  $48^{\circ}\text{W}$  was not under the 2009 UTC SSM/I overpass. However, the

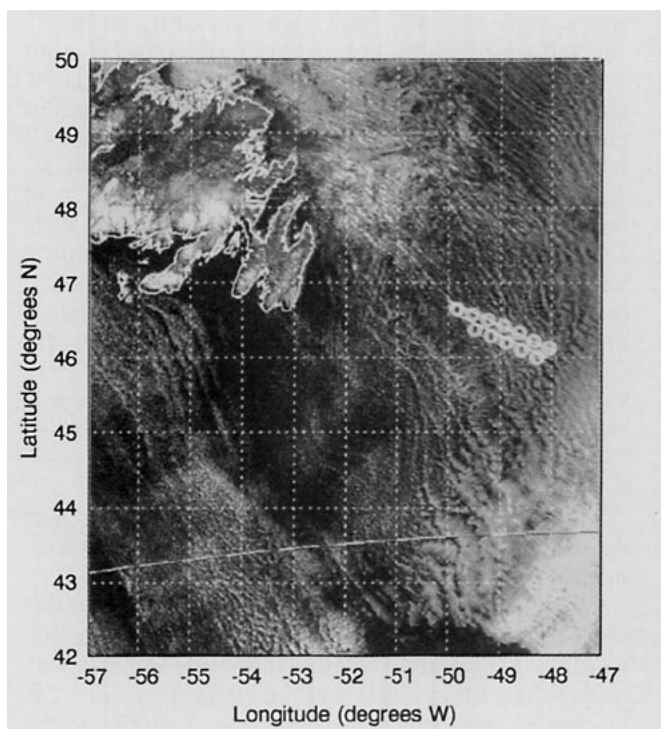


FIG. 9. NOAA-11 1830 UTC 15 February 1992 visible satellite image.

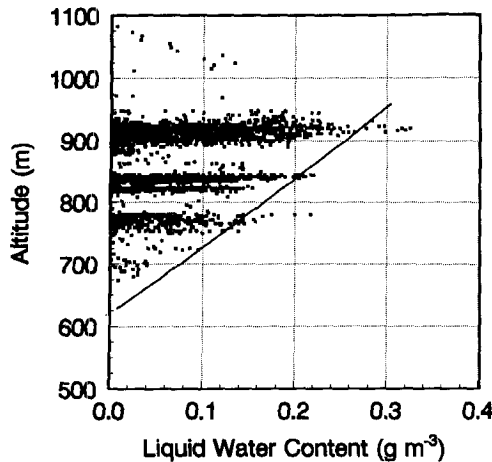


FIG. 10. Vertical profile of LWC measured with the aircraft between 2100 and 2300 UTC 15 February 1992.

flight track between  $50^{\circ}$  and  $48^{\circ}$ W was roughly 160 km long (Fig. 9), contained three full vertical profiles and long segments at three separate altitudes, and collectively should represent a good characterization of the streamer clouds in the region of the flight. This was further supported by NOAA visible and IR satellite images at 1830 and 2245 UTC, which showed that the clouds across the region of the flight appeared quite similar and that there was no significant change in the clouds with time.

The clouds were 320 m thick, with a cloud-base temperature of  $-9^{\circ}\text{C}$ , and were capped by an inversion at  $-15^{\circ}\text{C}$ . The clouds were supercooled with droplet concentrations of  $400\text{--}600\text{ cm}^{-3}$ , with crystal dendrites to 4-mm diameter observed throughout the cloud in concentrations of  $10\text{--}20\text{ L}^{-1}$ . Figure 10 shows the variation of SLWC with altitude for all data between 2100 and 2300 UTC. The LWC was highly stratified with altitude with peak 1-s SLWCs equaling their adiabatic values. The range of SLWC between zero and the adiabatic value reflects the aircraft flying through cloud patches separated by areas of clear air. The average LWP was  $0.010 \pm 0.006\text{ kg m}^{-2}$ , which is higher than the 11 February 1992 value but still close enough to zero to be similar to a clear-sky case. Averages of satellite data over 12 SSM/I pixels coincident with the flight track (Fig. 9) are listed in Table 3.

In general the LWP retrievals agreed with the aircraft measurements within the variability of the measurements ( $0.01\text{--}0.02\text{ kg m}^{-2}$ ). The results from the *F-10* satellite at 2009 UTC and *F-11* satellite at 2320 UTC were very similar with LWP measurements, agreeing within  $0.002\text{ kg m}^{-2}$  for most of the algorithms. This supports the observation that the cloud fields on a 25-km scale were unchanged over the duration of the flight.

f. Case 5, 1 March 1992: Thick, highly glaciated streamer clouds

An intense low pressure center was located north east of Newfoundland on 1 March 1992. Thick streamer clouds formed in the  $25\text{ m s}^{-1}$  westerly surface winds that were associated with the circulation around the low. Figure 11 shows the 1717 UTC NOAA-12 satellite image. A similar image from the 2230 UTC NOAA-12 satellite showed that the cloud fields were virtually unchanged. Both satellite measurements gave cloud-top temperatures of  $-30^{\circ}\text{C}$  across the flight area. A research flight (Fig. 11) was conducted to the east of St. John's with the intention of measuring heat and mass fluxes across the sea ice-ocean boundary. Although most of the flight was conducted below cloud base, good vertical profiles through the cloud were made at 1700 and 1800 UTC. An *F-11* SSM/I overpass occurred at 2017 UTC, which was about 2 hours after the aircraft measurements. However, because of the persistence of the clouds, it was felt that the aircraft and SSM/I measurements could be compared. Three aircraft profiles were made from cloud base to cloud top, with in-cloud horizontal scales between 19 and 26 km. Thus the aircraft measurements of the clouds were over a scale roughly equal to the 37-GHz SSM/I pixel size and should be suitable for comparison.

The streamers were well developed with cloud base at 850 m and cloud top at 1650 m. The clouds had high ice crystal concentrations from  $130\text{ to }250\text{ L}^{-1}$ , and some crystal and snow showers were observed below

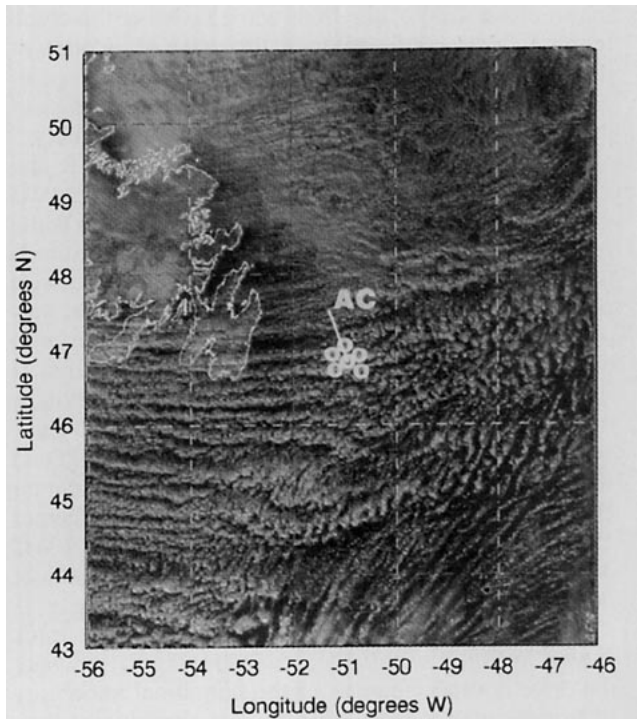


FIG. 11. NOAA-11 1717 UTC 1 March 1992 visible satellite image.

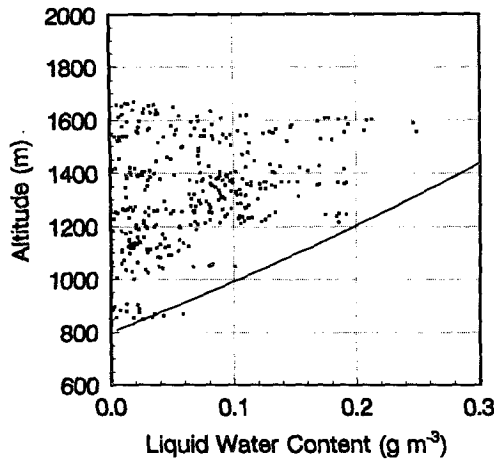


FIG. 12. Vertical profile of LWC measured with the aircraft on 1 March 1992.

cloud base during the flight. Figure 12 shows the liquid water profile with altitude for the three profiles. Liquid water was observed throughout the cloud with maximum values near cloud top of  $0.25 \text{ g m}^{-3}$  (0.65 of the adiabatic value). The SLWC was coincident with the ice crystals, which was somewhat surprising given the high ice crystal concentrations and cold cloud temperatures. It is likely that regions of SLWC were being driven by the strong surface winds picking up moisture from the ocean surface. These supercooled regions were then gradually glaciated, with crystal showers forming a moisture sink from the clouds.

SSM/I averages were taken from seven SSM/I pixels that corresponded to the areas around the portion of the flight track over the open ocean and away from the sea ice (Fig. 11). Given that the clouds were 800 m thick, a continuous cloud LWC profile, at 0.65 of the adiabatic value, to  $0.24 \text{ g m}^{-3}$  at cloud top would have given a LWP of  $0.096 \text{ kg m}^{-2}$ . However, the aircraft LWP was  $0.032 \pm 0.009 \text{ kg m}^{-2}$ , which is indicative of the glaciated nature of the clouds. While the LWP algorithms based on radiative transfer models (Liu and Curry; Greenwald) agreed closely with the aircraft measurements, the Alishouse and Petty algorithms appeared to significantly overestimate the LWP in this case. Surface stations indicated wind speeds of  $25 \text{ m s}^{-1}$ , while the aircraft-measured TPW for altitudes below 6.8 km was  $2.3 \text{ kg m}^{-2}$ . Both measurements are extreme values and may explain the poor performance of the latter LWP algorithms. This will be discussed in section 6.

*g. Case 6, 17 February 1992: Warm front region stratus clouds*

On 17 February 1992, a research flight was conducted into a cloud region near a low pressure center. A spiral vertical profile at 1300 UTC, through cloud

associated with a warm front, coincided with a 1240 UTC SSM/I *F-10* overpass. Since the measurements were over the ocean and most of the aircraft spiral descent had a diameter between 13 and 26 km, this was considered a good case for comparison of SSM/I and aircraft data. It was the only comparison case available from CASP II where the cloud was associated with a synoptic feature. Figure 13 shows the 1218 UTC NOAA-12 visible image with the location of the aircraft and SSM/I measurements superimposed. A stratiform deck is visible with a cloud-top temperature of  $-10^\circ\text{C}$ , although portions of the deck have been obscured by higher cirrus clouds. The aircraft did not measure the cirrus cloud, although two ice crystal showers from the cirrus were measured prior to the descent. Two distinct cloud layers were measured during the aircraft vertical descent from 6 km to 300 m. These can be seen in the LWC altitude profile shown in Fig. 14. The upper layer had SLWCs to  $0.33 \text{ g m}^{-3}$  at cloud top, with the cloud below being partially glaciated and having much lower SLWCs. Ice crystals were mainly plates smaller than 0.5 mm, with concentrations between 0.1 and  $0.5 \text{ L}^{-1}$ . The maximum SLWCs observed were consistent with a 400-m-deep adiabatic profile; however, only the cloud-top region could be considered close to adiabatic. The lower cloud had maximum LWCs of  $0.2 \text{ g m}^{-3}$  near cloud base, with higher crystal concentrations of  $150\text{--}250 \text{ L}^{-1}$  (crystals larger than 0.1 mm). The crystals in the lower cloud were primarily needles, plates,

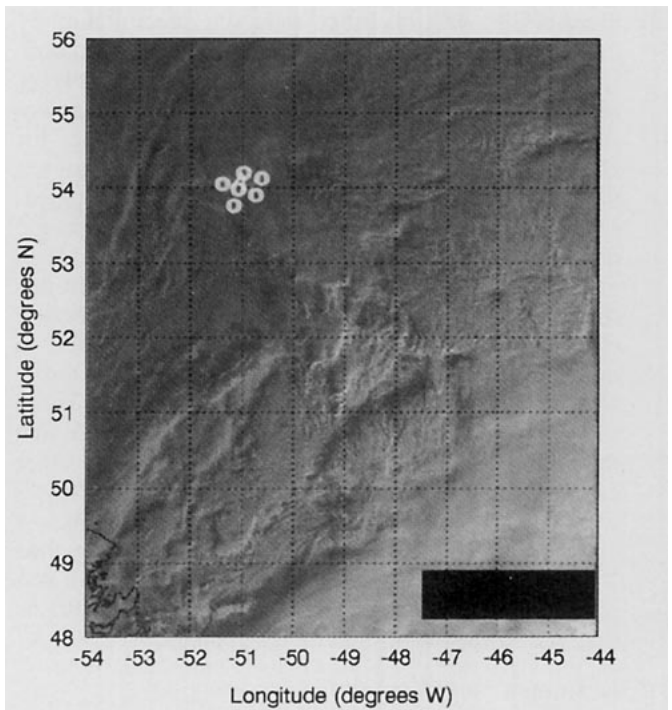


FIG. 13. NOAA-12 1218 UTC 17 February 1992 visible satellite image. The aircraft flight track is centered on the middle SSM/I pixel.

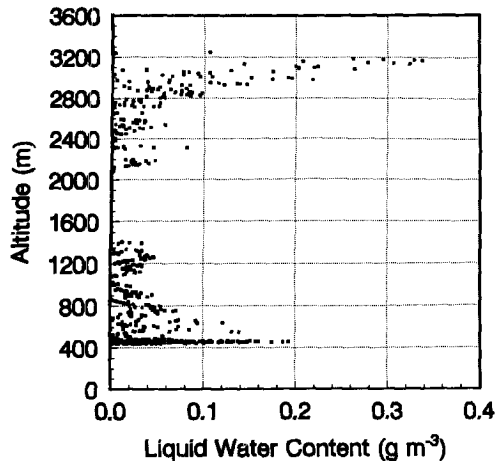


FIG. 14. Vertical profile of LWC measured with the aircraft between 1245 and 1315 UTC 17 February 1992.

and needle aggregates, with the latter observed as large as 6 mm in diameter.

The LWP retrieval fields for Liu and Curry (37V) in the region of the aircraft profile are shown in Fig. 15. Although most of the aircraft LWC data coincided with two SSM/I pixels, the aircraft crossed part of five pixels during the profile through the cloud. These five pixels are indicated in Figs. 13 and 15. The sea ice edge was far enough to the west that no effect should be evident for the pixels coinciding with the aircraft profile. Regions to the northeast, west, and south of the flight profile were classified as having precipitation by the Goodberlet algorithm. The aircraft LWP from both cloud layers was  $0.09 \pm 0.02 \text{ kg m}^{-2}$ . The cirrus layer above was at temperatures below  $-30^\circ\text{C}$  and was not suspected to have any LWC. There was a tendency for all the algorithms to overestimate the LWP by between  $0.03$  and  $0.09 \text{ kg m}^{-2}$ , as compared to the aircraft measurement. Because there was only one vertical profile through the cloud, it is possible that the aircraft data was not completely representative of the cloud in this region. The SSM/I LWP measurements showed a sharper gradient in the flight region than existed in other case studies. This is evident from the variability of the SSM/I LWPs, which was  $0.04 \text{ kg m}^{-2}$  for the five pixels covering the flight region, suggesting that the clouds were not as homogeneous as in the other cases. It is unlikely that the satellite LWP retrievals were larger because of liquid phase precipitation below cloud base. The surface temperature was cooler than  $0^\circ\text{C}$  (as measured with four dropsondes), so there was no possible influence on the LWP from rain or drizzle that had formed from melted ice crystals.

## 6. Comparison of results

A summary of SWS, TPW, and LWP measurements and retrievals for each of the six case studies is given

in Table 3. Although there are insufficient data points for a statistical analysis, trends and differences in the algorithms are evident from scatterplots comparing the aircraft and satellite measurements.

### a. Total precipitable water

While comprehensive comparisons of TPW have been made by other authors, given the potential dependence of TPW on LWP, it was necessary to verify the TPW algorithms for the six comparison cases. Figures 16a–d show comparisons between the aircraft and dropsonde measurements of TPW and retrieved TPW from the Petty, modified Petty, Alishouse, and Greenwald algorithms, respectively. On average, the aircraft–dropsonde data would be expected to be underestimated because altitudes above 6.5 km were never sampled. A further error can occur for aircraft-derived TPW since the TPW from the surface to the lowest altitude reached over the ocean by the aircraft must be estimated. In general,  $\pm 0.5 \text{ kg m}^{-2}$  is a reasonable error estimate for aircraft- or dropsonde-derived TPW. The variability of SSM/I TPW was always less than  $1 \text{ kg m}^{-2}$ , which was smaller than the minimum rms errors of  $2\text{--}3 \text{ kg m}^{-2}$  given by Alishouse et al. (1990a). The Petty results show excellent agreement with the aircraft data, agreeing within the experimental error for all six data points. The modified Petty measurements showed similar agreement with the aircraft data, with the exception of case 5, where the agreement was worse. The Alishouse results are similar for TPW greater than  $5 \text{ kg m}^{-2}$ . However, for case 5 where the TPW was  $2.3 \text{ kg m}^{-2}$ , the algorithm overestimated the TPW. This problem has been previously recognized (Hollinger 1991), where it was shown that the algo-

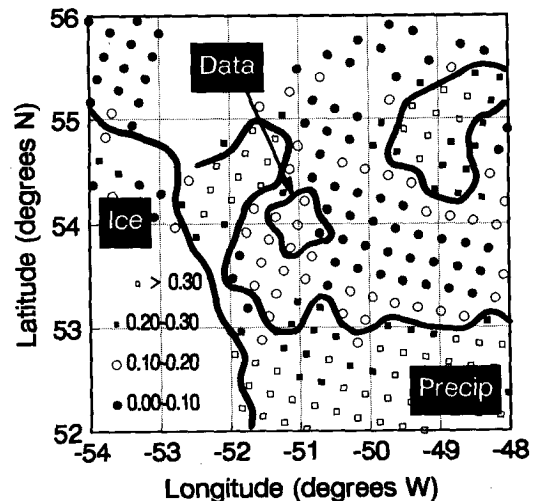


FIG. 15. SSM/I measurement of LWP ( $\text{kg m}^{-2}$ ) from the Liu and Curry 37V algorithm for 17 February 1992. Markings are as in Figs. 3 and 6.

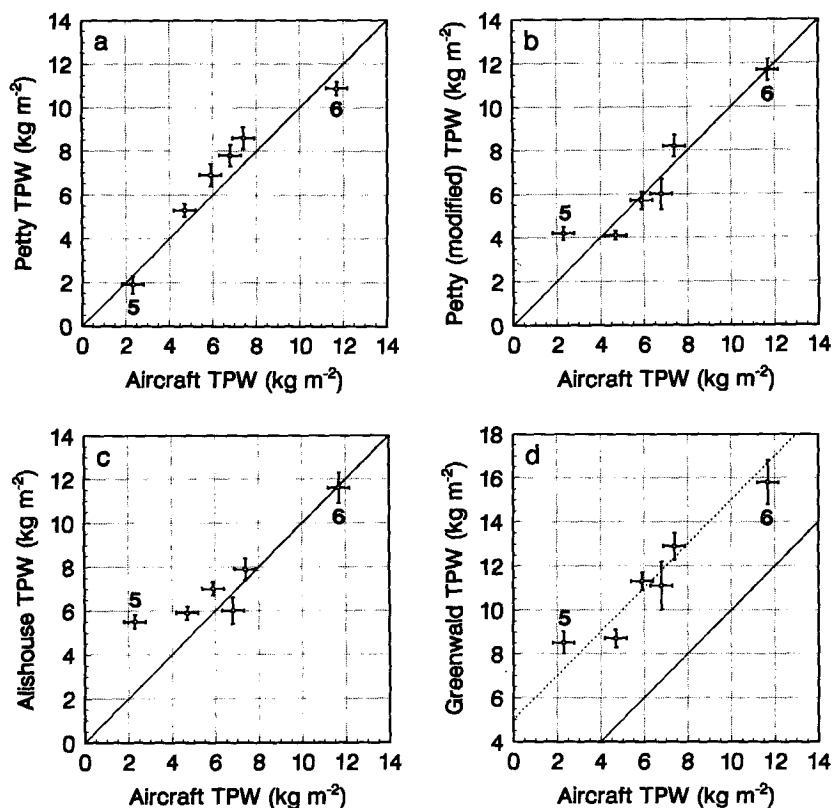


FIG. 16. Comparison of total precipitable water measured from the aircraft or dropsondes and those calculated from the following algorithms: (a) Petty; (b) modified Petty; (c) Alishouse; (d) Greenwald. The dotted curve in (d) represents a 1:1 correlation with a systematic shift of 5 kg m<sup>-2</sup> in the y axis.

gorithm tended to level off at about 5 kg m<sup>-2</sup> for real TPW values less than 5 kg m<sup>-2</sup>. The Greenwald retrievals showed a significant systematic bias of  $5 \pm 2$  kg m<sup>-2</sup>, which was surprising given the good agreement of the Greenwald LWP algorithm (Section 6b). It is unclear why the Greenwald algorithm was systematically in error.

#### b. Liquid water path

Comparisons between LWP retrievals from nine algorithms and aircraft data are shown in Figs. 17a–i. Case numbers requiring special attention are indicated on each of the graphs. Each curve will be discussed in detail below. As indicated in section 5g, each algorithm showed poor agreement with the aircraft measurements for case 6 (17 February 1992). This point was not considered when determining the best fits and will be discussed separately below.

The Alishouse 6, 4h, and 4l graphs (Figs. 17a–c) are very similar, with a best fit (dashed lines) within 0.01 kg m<sup>-2</sup> of the 1:1 correlation curve. Each algorithm performed poorly for case 5 (1 March 1992), and this point was not considered when determining the

best fits. The 6 and 4h channel retrievals showed a small systematic bias of 0.01 kg m<sup>-2</sup>, while the 4l-channel retrievals showed a systematic bias of  $-0.01$  kg m<sup>-2</sup>. The similarities between the algorithms was not surprising, given that all three use linear combinations of 19-, 22-, and 37-GHz data, while the 6 and 4h algorithms also use 85-GHz data. The agreement between aircraft and SSM/I measurements was 0.02–0.03 kg m<sup>-2</sup>, which was better than the 0.04 kg m<sup>-2</sup> accuracy quoted by Alishouse et al. (1990b). Conversely, the Alishouse one-channel retrievals (Fig. 17d) showed a  $-0.05$  kg m<sup>-2</sup> systematic shift.

In case 5, the SWS was 25 m s<sup>-1</sup>, which is quite high and can be considered extreme, while the TPW was 2.3 kg m<sup>-2</sup>, which is quite low and can also be considered extreme. Given the dependence of the Alishouse TPW and Goodberlet SWS on 19-, 22-, and 37-GHz data, extreme values of TPW and SWS indicate extreme brightness temperatures. The linear dependence of the Alishouse LWP algorithm on 19-, 22-, and 37-GHz data may not be sufficient in such cases. It is unlikely that the 20 data points used in the original fits of Alishouse et al. (1990b) contained many cases with extreme values of SWS and TPW. Therefore,

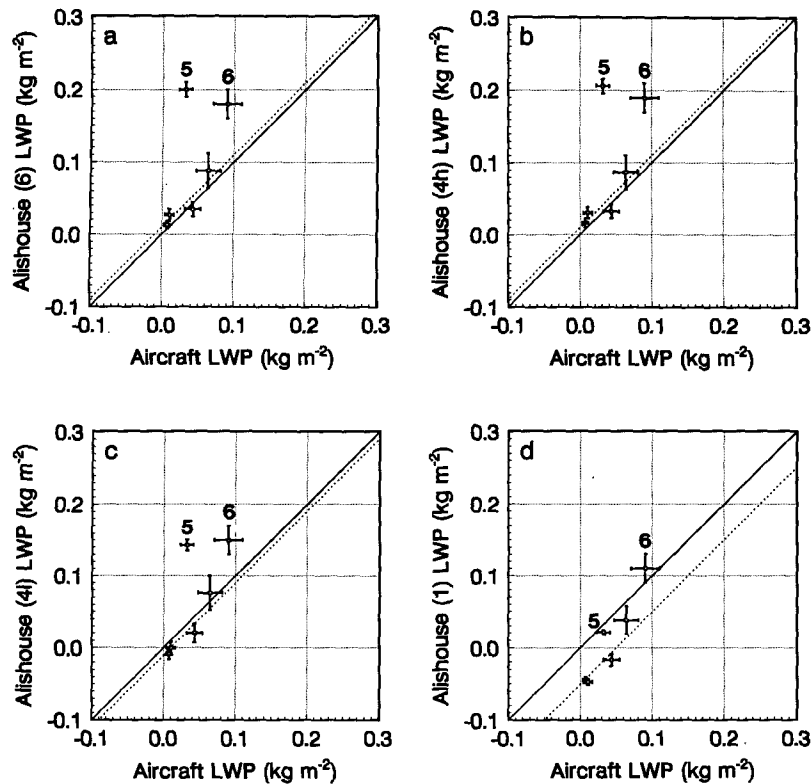


FIG. 17. Comparison of liquid water path measured from the aircraft with those from the following algorithms: (a) Alishouse 6 channel; (b) Alishouse 4h channel; (c) Alishouse 4l channel; (d) Alishouse 1 channel; (e) Petty; (f) modified Petty; (g) Liu and Curry 37H; (h) Liu and Curry 37V; (i) Greenwald. Solid lines represent 1:1 correlations, while dotted lines show 1:1 correlations with a systematic shift along the y axis.

given the potential correlations between SWS, TPW, and LWP, it was not surprising to see the algorithm work poorly for case 5. This was further supported by the fact that the Liu and Curry and Greenwald algorithms, which are physically based, gave results consistent with the aircraft measurements, while the Petty algorithm, which incorporates direct dependencies of SWS and TPW on LWP, gave similar results to the Alishouse algorithms. This suggests that the algorithms based on radiative transfer models are better able to uncouple LWP, SWS, and TPW and can better represent situations with extreme brightness temperatures.

The Petty original and modified LWP algorithm comparisons (Figs. 17e–f) showed systematic shifts of 0.06 and 0.04  $\text{kg m}^{-2}$ , respectively, from the 1:1 correlation curve. The systematic differences exceeded the accuracy of the Petty algorithms and will be discussed below. However, the shifted curves agreed with the aircraft measurements within the minimum rms error of 0.025  $\text{kg m}^{-2}$  quoted by Petty (1990). The variability in each data point was reduced in the modified Petty algorithm. The modified LWP algorithm also gave good agreement for case 5, suggesting that the modified algorithms were more effective in separating SWS, TPW, and LWP.

Aircraft comparisons with the Liu and Curry 37H and 37V retrievals are shown in Figs. 17g and 17h, respectively. Case 5 was well handled by both algorithms. There was a systematic shift in the 37H and 37V algorithms of  $-0.01$  and  $-0.02 \text{ kg m}^{-2}$ , respectively. Although Liu and Curry preferred the 37H algorithm, the 37V algorithm appeared to provide a better fit to the aircraft data than the 37H algorithm. Accounting for the systematic shift, the 37V algorithm gave the best fit to the aircraft data of the nine LWP algorithms, with all points agreeing with the aircraft data within 0.02  $\text{kg m}^{-2}$ .

Figure 17i shows a comparison of the aircraft data with the Greenwald LWP retrievals. This algorithm also performed well for the 1 March 1992 case. There was no systematic bias in the LWP measurements, with aircraft and SSM/I measurements agreeing within 0.02  $\text{kg m}^{-2}$ . However, the large systematic bias in the TPW raises concerns about the LWP since they are solved simultaneously in the Greenwald algorithms, and any tuning that would bring the TPW toward more reasonable values would also shift the LWP. Greenwald et al. (1993) did not show any TPW comparisons, and it is unclear whether they had similar observations.

A distinct feature evident in Figs. 17a–i is the systematic shifts in the SSM/I measurements that appear

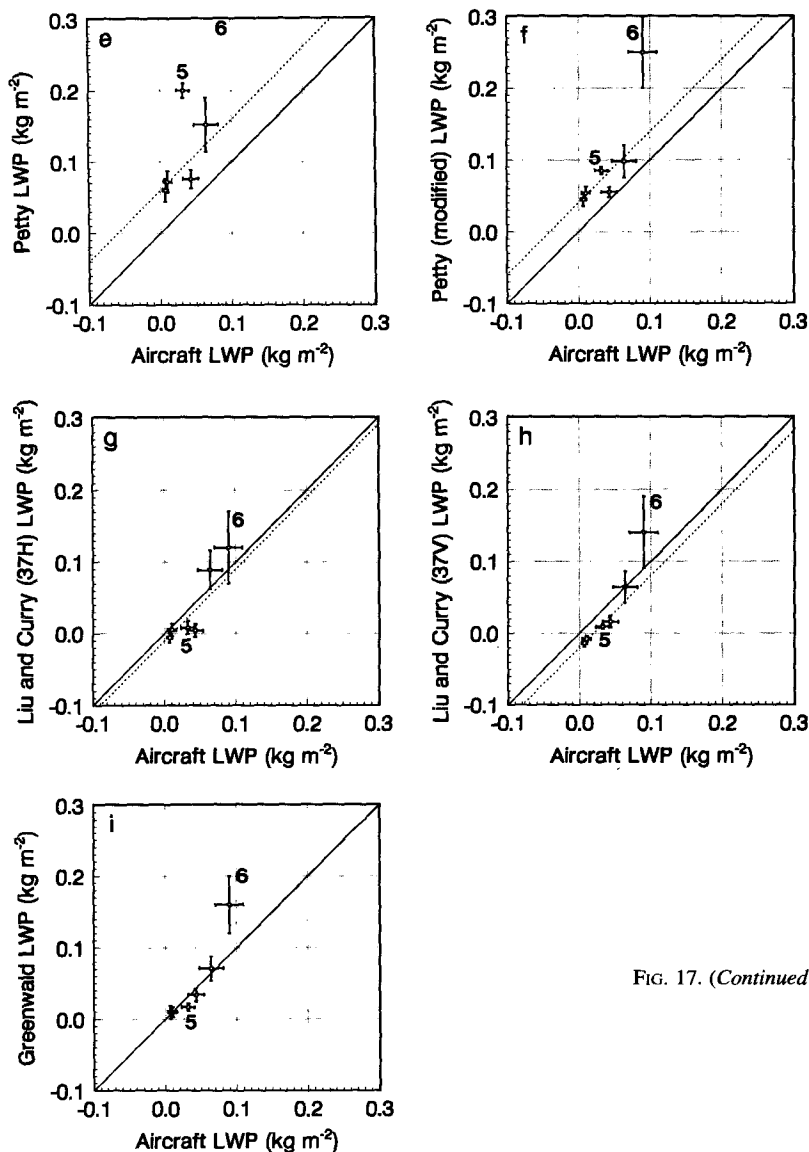


FIG. 17. (Continued)

necessary to get an optimum agreement with the aircraft measurements. These shifts ranged from  $-0.06 \text{ kg m}^{-2}$  for the Petty algorithm to  $0.05 \text{ kg m}^{-2}$  for the Alishouse one-channel algorithm. It is suspected that these shifts are related to regional (latitudinal and seasonal) effects. The Alishouse and Petty algorithms were based on ground-based measurements from San Nicolas Island ( $33^\circ\text{N}$ , measurements during the summer) and Kwajalein Island ( $8^\circ\text{N}$ , measurements during the winter/spring), while the measurements reported here are from  $45^\circ$  to  $55^\circ\text{N}$  during the winter. Local conditions of sea surface emissivity and mean atmospheric or cloud temperature would be inherent in these algorithms and may cause the algorithms to be biased when used in other regions. Liu and Curry (1993) indicated that the Alishouse algorithm may not be representative

for latitudes and seasons outside those from where the ground-validation measurements were taken. The algorithms based on radiative transfer models may also have slight regional biases. These models are generally tuned to give zero LWP values in clear-sky cases and may inherit a small regional bias in the tuning process. The aircraft measurements show that most of the algorithms had a systematic bias of less than  $0.02 \text{ kg m}^{-2}$ . The biases observed for the Petty algorithms suggest that caution is necessary before applying these algorithms to northern winter cases. The Alishouse algorithms were based on the same original dataset, although the systematic shift in the one-channel algorithm is in the opposite direction to that for the Petty algorithm. The different approaches used for deriving these algorithms likely accounts for the different biases.

Accounting for the systematic biases, the Greenwald, Liu and Curry, and Alishouse algorithms gave LWP retrievals between  $0.15 \pm 0.03 \text{ kg m}^{-2}$  for case 6. This was 60% higher than the aircraft measurements and indicated that either the aircraft underestimated the LWP or the SSM/I algorithms collectively overestimated LWP. There is sufficient doubt about the aircraft data in this case to discount this point in the satellite comparison. However, the Greenwald and Liu–Curry algorithms showed closer agreement to the aircraft measurements than the Alishouse or Petty algorithms. The physically based algorithms also showed a stronger LWP gradient through the aircraft measurement region and higher LWP variability than the other algorithms. Consequently, the LWP measurements of Liu and Curry and Greenwald were much more consistent with the aircraft data than the Alishouse and Petty algorithms. This can be clearly seen in Fig. 17.

### c. Scattering index comparison

It is recognized that ice crystals can cause significant scattering of microwaves at 85 and 37 GHz, while the effects of ice crystal scattering on the 19- and 22-GHz channels are generally negligible (Grody 1993). While scattering effects were not expected to affect the TPW or SWS measurements in the case studies described above (since the dominating terms in the algorithms used 19- and 22-GHz brightness temperatures), there was some concern that the LWP measurements could be contaminated by scattering since they relied primarily on the 37- and 85-GHz brightness temperatures. The scattering index of Grody (1993) was calculated for the 85- and 37-GHz channels for the SSM/I pixels used in each comparison. These values physically represent the possible change in brightness temperature caused by scattering from ice particles. Grody notes that positive values larger than 7 and 10 K (for 37- and 85-GHz indexes, respectively) are indicative of significant scattering. Figures 18a and 18b show the scattering indexes versus LWP for each case. The scattering indexes were negative and showed a direct dependence on LWP. This indicates that the scattering index measured only the effect of LWP on the 37 and 85 frequencies (i.e., emission effects and not scattering effects) and that ice crystal concentrations measured in each case had no effect on the LWP measurements. Since the ice crystal spectra were generally exponential, the number of large crystals, and consequently the magnitude of the scattering, should be proportional to the concentration. Although the clouds were classified as nonprecipitating clouds, ice crystal concentrations in cases 2, 5, and 6 exceeded  $50\text{--}100 \text{ L}^{-1}$  over a depth of 1 km, with crystal showers reaching the surface in case 5. The lack of any scattering signal from the scattering index for these cases suggests that the scattering index should not be used to discount the existence of ice in similar cloud systems in northern winter storms.

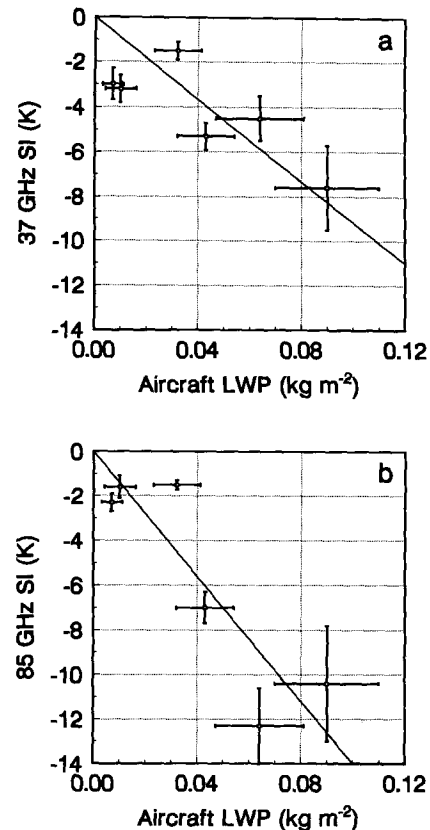


FIG. 18. Scattering index (SI), as based on Grody (1993), versus LWP for the following indexes: (a) 37 GHz; (b) 85 GHz. The curves represent linear best fits.

## 7. Conclusions

In situ measurements of liquid water path have been made from a research aircraft that was fully instrumented for cloud microphysics measurements. The measurements have been compared to coincident measurements from the DMSP SSM/I. Comparisons from six cases allow the following conclusions.

- 1) The Petty (1990) algorithm for total precipitable water gave results that agreed with the aircraft measurements within their respective errors. The Alishouse et al. (1990a) algorithm gave results that agreed when the TPW exceeded  $5 \text{ kg m}^{-2}$ , although it overestimated the TPW for a case where the TPW was  $2.3 \text{ kg m}^{-2}$ . The Greenwald et al. (1993) algorithm systematically overestimated the TPW by  $5 \pm 2 \text{ kg m}^{-2}$ .

- 2) While it is recognized that the conclusions are limited by the small dataset, the liquid water path algorithms of Petty (1990), Alishouse et al. (1990b), Liu and Curry (1993), and Greenwald et al. (1993) showed either good agreement or systematic differences with the aircraft data for most cases. When the systematic differences were taken into account, the retrieved data agreed with the aircraft measurements

within  $\pm 0.02$ – $0.03 \text{ kg m}^{-2}$ , which was similar to the accuracies quoted by the authors. However, for some algorithms these biases were as high as  $\pm 0.06 \text{ kg m}^{-2}$ . It is believed that such biases are caused by latitudinal and seasonal effects that are inherent in the algorithms. For any algorithm, clear-sky measurements might be used to quantify the systematic bias for specific regions and seasons.

3) The algorithms based on radiative transfer models appeared to give better results than the algorithms based on statistical techniques. This was particularly true for one case study where the surface winds and total precipitable water were considered extreme. It is suggested that the correlations between LWP, TPW, and SWS are better handled in the model-based algorithms. Assuming that zero LWP (clear sky) cases can be correctly defined, the aircraft comparisons support the claims of Greenwald et al. (1993) and Liu and Curry (1993) that the LWP algorithms are capable of measuring LWP to within  $\pm 0.02 \text{ kg m}^{-2}$ .

4) The results presented here demonstrate that in situ aircraft measurements can be used to validate, improve, and intercompare satellite-based LWP retrieval algorithms. Previous validations of SSM/I LWP algorithms have only been performed by comparisons with upward-looking radiometers and calculations with radiative transfer models, and the examples presented here reflect an alternative technique for validation.

*Acknowledgments.* Funding for this research was provided by the Canadian National Search and Rescue Secretariat. Funding for the field project was also provided by the Atmospheric Environment Service (AES), Institute of Aerospace Research (IAR), Boeing Commercial Airplane Group, Airbus Industrie, and the Panel of Energy Mines and Resources. Boeing funding was specifically dedicated to SSM/I validation research flights. The authors would like to acknowledge Ron Stewart, Walter Strapp, and Mike Patnoe for their knowledge, support, and assistance during the field project. The Satellite Meteorology Division at AES, and particularly Alex Aldunate, is acknowledged for their considerable assistance in analyzing the NOAA satellite images. Thanks also to Anna Glazer for setting up the programs for processing LWP retrievals. Finally, the technicians and programmers of AES and IAR are acknowledged for their support on keeping the aircraft, instruments, and data systems operational.

## REFERENCES

- Alishouse, J. C., S. A. Snyder, J. Vongsathorn, and R. R. Ferraro, 1990a: Determination of oceanic total precipitable water from the SSM/I. *IEEE Trans. Geosci. Remote Sens.*, **28**, 811–816.
- , J. B. Snider, E. R. Westwater, C. T. Swift, C. S. Ruf, S. A. Snyder, J. Vongsathorn, and R. R. Ferraro, 1990b: Determination of cloud liquid water content using the SSM/I. *IEEE Trans. Geosci. Remote Sens.*, **28**, 817–821.
- Cober, S. G., G. A. Isaac, and J. W. Strapp, 1995: Aircraft icing measurements in East Coast winter storms. *J. Appl. Meteor.*, **34**, 88–100.
- Colton, M. C., and G. A. Poe, 1994: Shared processing program, Defense Meteorological Satellite Program, Special Sensor Microwave/Imager algorithm symposium, 8–10 June 1993. *Bull. Amer. Meteor. Soc.*, **75**, 1663–1669.
- Curry, J. A., and G. Liu, 1992: Assessment of aircraft icing potential using satellite data. *J. Appl. Meteor.*, **31**, 605–621.
- , C. D. Ardeel, and L. Tian, 1990: Liquid water content and precipitation characteristics of stratiform clouds as inferred from satellite microwave measurements. *J. Geophys. Res.*, **95D**, 16 659–16 671.
- Goodberlet, M. A., C. T. Swift, and J. C. Wilkerson, 1989: Remote sensing of ocean surface winds with the special sensor microwave/imager. *J. Geophys. Res.*, **94C**, 14 547–14 555.
- , —, and —, 1990: Ocean surface wind speed measurements of the special sensor microwave/imager (SSM/I). *IEEE Trans. Geosci. Remote Sens.*, **28**, 823–827.
- Greenwald, T. J., G. L. Stephens, T. H. Vonder Haar, and D. L. Jackson, 1993: A physical retrieval of cloud liquid water over the global oceans using special sensor microwave/imager (SSM/I) observations. *J. Geophys. Res.*, **98D**, 18 471–18 488.
- Grody, N. C., 1993: *Atmospheric Remote Sensing by Microwave Radiometry*. M. A. Janssen, Ed., J. Wiley and Sons Inc., 572 pp.
- Hollinger, J. P., Ed., 1991: Defense meteorological satellite program special sensor microwave/imager calibration/validation. Vol. II. Naval Research Laboratory Tech. Rep., 304 pp.
- , J. L. Peirce, and G. A. Poe, 1990: SSM/I instrument evaluation. *IEEE Trans. Geosci. Remote Sens.*, **28**, 781–789.
- Lee, T. F., J. R. Clark, and S. D. Swadley, 1994: Potential applications of the SSM/I cloud liquid water parameter to the estimation of marine aircraft icing. *Wea. Forecasting*, **9**, 173–182.
- Liu, G., and J. A. Curry, 1993: Determination of characteristic features of cloud liquid water from satellite microwave measurements. *J. Geophys. Res.*, **98D**, 5069–5092.
- Patnoe, M. W., W. G. Tank, G. A. Isaac, S. G. Cober, and J. W. Strapp, 1993: Airplane icing research at the Boeing Company: Participation in the Canadian Atlantic Storms Program. Preprints, *Fifth Int. Conf. on Aviation Weather Systems*, Vienna, VA, Amer. Meteor. Soc., 432–434.
- Petty, G. W., 1990: On the response of the Special Sensor Microwave/Imager to the marine environment—Implications for atmospheric parameter retrievals. Ph.D. thesis, University of Washington, 291 pp.
- , and K. B. Katsaros, 1992: *Nimbus-7 SMMR precipitation observations calibrated against surface radar during TAMEX*. *J. Appl. Meteor.*, **31**, 489–505.
- Prigent, C., A. Sand, C. Klapisz, and Y. Lemaitre, 1994: Physical retrieval of liquid water contents in a North Atlantic cyclone using SSM/I data. *Quart. J. Roy. Meteor. Soc.*, **120**, 1179–1207.
- Stewart, R. E., 1991: Canadian Atlantic Storms Program: Progress and plans of the meteorological component. *Bull. Amer. Meteor. Soc.*, **72**, 364–371.